

MINI-RF X-BAND BISTATIC OBSERVATIONS OF THE MOON. G. W. Patterson¹, J. T. S. Cahill¹, L. M. Carter², G. A. Morgan³, C. D. Neish⁴, M. C. Nolan², D. M. Schroeder⁵, M. A. Slade⁶, A. M. Stickle¹, B. J. Thomson⁷, and the Mini-RF team, ¹Johns Hopkins University Applied Physics Laboratory, Laurel, MD (Wes.Patterson@jhuapl.edu). ²Lunar and Planetary Laboratory, Tucson AZ. ³Planetary Science Institute, Tucson AZ. ⁴University of Western Ontario, London, ON, Canada. ⁵Stanford University, Stanford CA. ⁶Jet Propulsion Laboratory, Pasadena CA. ⁷The University of Tennessee, Knoxville TN.

Introduction: NASA's Mini-RF instrument on the Lunar Reconnaissance Orbiter (LRO) is currently operating in concert with the Goldstone deep space communications complex 34 meter antenna DSS-13 to collect bistatic radar data of the Moon. These data provide a means to characterize the scattering properties of the upper meter of the lunar surface, as a function of bistatic angle, at X-band wavelengths (4.2 cm) and are being collected to address LRO science objectives related to: the vertical distribution of lunar water; the form and abundance of lunar water ice; how impacts expose and break down rocks to produce regolith on the Moon and other airless bodies; the present rate of regolith gardening; and how lunar volcanism has evolved over time.

Background: For each bistatic observation, the lunar surface is illuminated with a circularly polarized, chirped signal that tracks the Mini-RF antenna boresight intercept on the surface of the Moon. The receiver operates continuously and separately receives the horizontal and vertical polarization components of the signal backscattered from the lunar surface. The resolution of the data is ~100 m in range and ~2.5 m in azimuth but can vary from one observation to another, as a function of the viewing geometry. For analysis, the data are averaged in azimuth to provide a spatial resolution of 100 m. This yields an ~25-look average for each sampled location.

The data returned provide information on the structure (i.e., roughness) and dielectric properties of surface and buried materials within the penetration depth of the system (up to ~50 cm) [1-4]. The bistatic architecture allows examination of the scattering properties of a target surface for a variety of bistatic angles. Laboratory data and analog experiments, at optical wavelengths, have shown that the scattering properties of lunar materials can be sensitive to variations in bistatic angle [5-7].

Operations: Collecting data in the Mini-RF bistatic architecture requires significant advance planning with both the LRO operations team and ground-based facilities. As a result, no more than a few collects per month are feasible. The current X-band bistatic campaign (2017-present) includes 72 observations of the lunar nearside and poles (Fig. 1). A variety of lunar terrains have been, and are being, targeted to address science objectives for the ongoing LRO extended

mission. These include collecting data of: Copernican crater ejecta blankets to characterize rates of regolith weathering; the ejecta of newly-formed craters to characterize the size and density distribution of wavelength-scale scatters as a function of distance from the impact; mare materials within the Imbrium basin to provide information on the locations, extents, and depths of flow units and deposits; irregular mare patches (IMPs) and pyroclastic deposits to characterize their radar properties and thickness; and the floors of south polar craters to search for signatures indicative of the presence of water ice. In concert with the collection of these data, modeling work is being conducted to characterize the response of surface materials to variations in incidence angle [8,9]. These data are available through the Washington University in St. Louis PDS Geosciences node (<https://pds-geosciences.wustl.edu/missions/lro/default.html>).

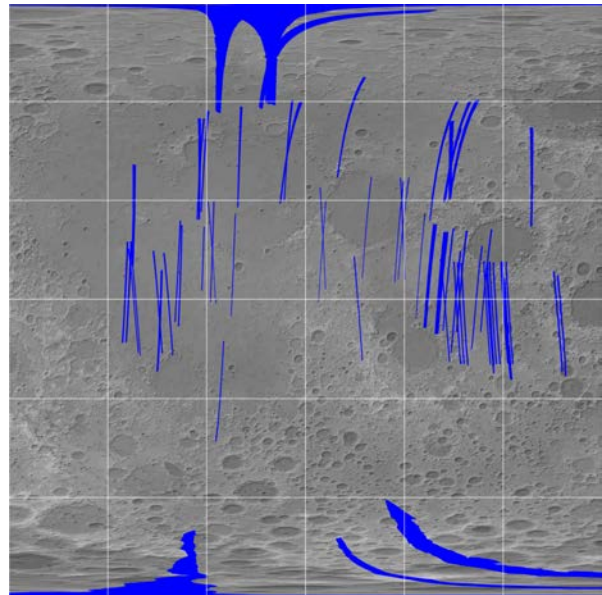


Fig. 1. Mini-RF bistatic X-band radar coverage (blue) for the lunar nearside (90°W to 90°E).

Initial Results: Analysis of available X-band data have provided new insights regarding impact, volcanic, and polar processes. Observations of Copernican crater ejecta materials show variations that can be attributed to the age of the crater. Differences between S- and X-band observations of the same crater are also present, providing new insight into the size-distribution of radar

scatterers within the ejecta [10]. Two craters that formed during the LRO mission have been identified in X-band Mini-RF data and analysis of these data suggest enhanced wavelength-scale surface roughness to radial distances of 100s of meters from the crater centers [11]. S- and X-band observations of mare materials in the Imbrium basin, combined with ground-based P-band observations, are providing important information on the locations, extents, and depths to individual flow units and deposits [12]. Analysis of south polar targets acquired at X-band do not appear to show the potential water ice signature detected at S-band [13,14]. This would indicate that, if water ice is present in Cabeus crater floor materials, it is buried beneath at least 0.5 m of regolith that does not include radar-detectable deposits of water ice.

Current Work: Recent targeted observations have focused on pyroclastic deposits associated with the Aristarchus Plateau and the Atlas thermophysical anomaly (Fig. 2). Data acquired of the Vallis Schröteri region of the plateau show distinct indications of secondary impact materials extending radially from Aristarchus crater (Fig. 2a, center). This is consistent with Mini-RF bistatic S-band [15,16] and ground-based bistatic S-band [17] observations of the region. These data, combined, provide information on the size and density distribution of centimeter- to decimeter-scale scatterers associated with secondary impact materials. Additionally, comparing the backscatter response of the margin of the pyroclastic deposit in X-, S-, and P-band data will provide important constrains on how the thickness of the deposit varies laterally. The Atlas thermophysical anomaly [18] is a region centered near $\sim 45^{\circ}\text{N}$, $\sim 45^{\circ}\text{E}$ and encompassing the craters Atlas, Hercules, Burg, and Keldysh. The region is characterized by unique thermophysical properties and distinct radar properties [19]. Mini-RF X-band bistatic data acquired over a portion of the region near the crater Keldysh show variations in backscattered power that may indicate differences in surface roughness or potential flow thickness (Fig. 2b, center). These data provide another piece to the puzzle that is this enigmatic region. Their comparison with radar data at S- and P-band will also provide useful information regarding the size and density distribution of centimeter- to meter-scale scatterers in the region.

Acknowledgments: This work is supported through a contract with the NASA Lunar Reconnaissance Orbiter mission.

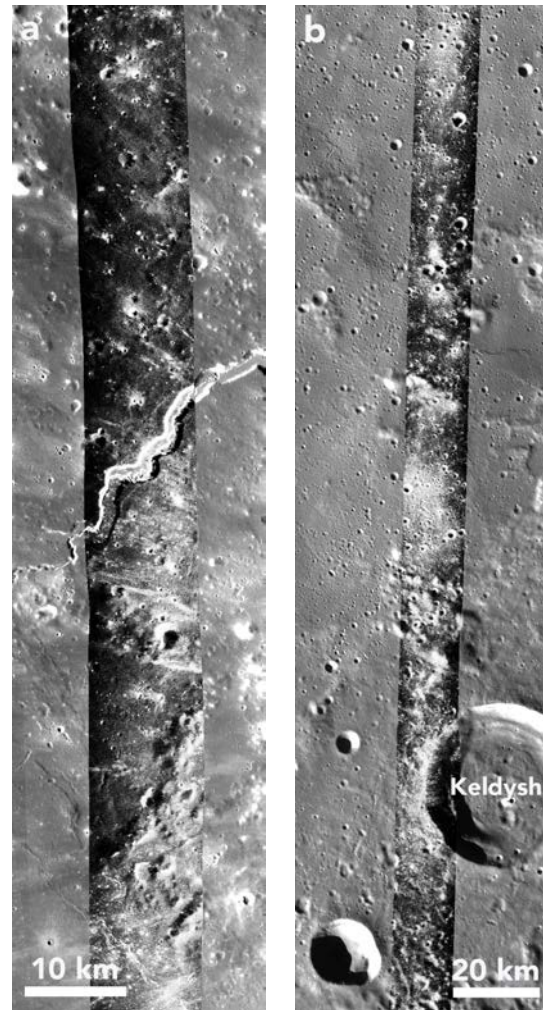


Fig. 2: Mini-RF X-band bistatic data covering (a) Vallis Schröteri on the Aristarchus plateau, acquired on March 7th, 2020, and (b) the Atlas thermophysical region [18], acquired on June 15th, 2020. These data are overlain on LROC WAC monochrome image data.

References: [1] Campbell et al. (2010), *Icarus*, 208, 565-573; [2] Raney et al. (2012), *JGR*, 117, E00H21; [3] Carter et al. (2012), *JGR*, 117, E00H09; [4] Campbell (2012), *JGR*, 117, E06008; [5] Hapke et al. (1998), *Icarus*, 133, 89-97; [6] Nelson et al. (2000), *Icarus*, 147, 545-558; [7] Piatek et al. (2004), *Icarus*, 171, 531-545. [8] Prem et al. (2020), *51st LPSC* #2099; [9] Virkki A. K. and Bhiravarasu S. S. (2019) *JGR*, E006006 [10] Stickle et al. (2019), *50th LPSC* #2937; [11] Cahill et al. (2018), *49th LPSC* #2693; [12] Morgan et al. (2020), *51st LPSC* #2733; [13] Patterson et al. (2019) *50th LPSC* #2861; [14] Patterson et al. (2017), *Icarus*, 283, 2-19; [15] Stickle et al. (2020), *51st LPSC* #2684; [16] Morgan et al. (2021), *52nd LPSC* #2512; [17] Campbell et al. (2008), *Geology*, 36(2), 135-138; [18] Hayne et al. (2017) *JGR*, 122, 2371; [19] Cahill et al. (2021), *52nd LPSC* #2114.